Trapping and manipulation of microparticles using laser-induced convection currents and photophoresis

E. Flores-Flores[a], S. A. Torres- Hurtado[b], R. Paez[b], U. Ruiz-Corona[b], G. Beltrán-Pérez[a], S.L. Neale[c], J.C. Ramirez-San-Juan[b], and R. Ramos-García[b*].

[a]*Benemérita Universidad Autónoma de Puebla, Calle 4 Sur 104 Colonia Centro, Puebla, Puebla, 72000, México.*

[b]*Instituto Nacional de Astrofísica, Óptica y Electrónica, Luis Enrique Erro No.1, Tonanzintla, Puebla, México.*

[c]University of Glasgow, James Watt South Building, Glasgow G12 8QQ, Scotland, UK

rgarcia@inaoep.mx

Abstract: In this work we demonstrate optical trapping and manipulation of microparticles suspended in water due to laser-induced convection currents. Convection currents are generated due to laser light absorption in an hydrogenated amorphous silicon (a:Si-H) thin film. The particles are dragged towards the beam's center by the convection currents (Stokes drag force) allowing trapping with powers as low as 0.8 mW. However, for powers >3 mW trapped particles form a ring around the beam due to two competing forces: Stokes drag and thermo-photophoretic forces. Additionally, we show that dynamic beam shaping can be used to trap and manipulate multiple particles by photophotophoresis without the need of lithographically created resistive heaters.

OCIS codes: (000.0000) General; (000.2700) General science.

References and links

1. A. Ashkin, "Optical trapping and manipulation of neutral particles using lasers," Proc. Natl. Acad. Sci. U.S.A. **94**(10), 4853–4860 (1997).
2. Ronald Pethig, "Review Article—Dielectrophoresis: Status of the theory, technology, and applications," Biomicrofluidics **4**(2), 022811 (2010).
3. P. Y. Chiou, A. T. Ohta, and M. C. Wu, "Massively parallel manipulation of single cells and microparticles using optical images," Nature **436**(7049), 7049 (2005).
4. M. Righini, A. S. Zelenina, C. Girard, and R. Quidant, "Parallel and selective trapping in a patterned plasmonic landscape," Nature Physics **3**(7), 477–480 (2007).
5. D. Psaltis, S. R. Quake, and C. H. Yang, "Developing optofluidic technology through the fusion of microfluidics and optics," Nature **442**(7101), 381–386 (2006).
6. K. Xiao, and D. G. Grier, "Sorting colloidal particles into multiple channels with optical forces: Prismatic optical fractionation", Phys. Rev. E **82**, 051407 (2010).
7. H. Melville, G. F. Milne, G. C. Spalding, W. Sibbett, K. Dholakia and D. McGloin, "Optical trapping of three-dimensional structures using dynamic holograms," Opt. Express **11**(26), 3409 (2003)
8. A. T. Ohta, A. Jamshidi, J. K. Valley, H.-Y. Hsu, and M. C. Wu, "Optically actuated thermocapillary movement of gas bubbles on an absorbing substrate," Appl. Phys. Lett. **91**(7), 074103 (2007).
9. W. H. Tan and S. Takeuchi, "A trap-and-release integrated microfluidic system for dynamic microarray applications," PNAS **104**(4), 1146–1151 (2007).
10. A. S. Basu, and Y. B. Gianchandani, "High speed microfluidic doublet flow in open pools driven by non-contact micromachined thermal sources," in *Proceedings of IEEE Conference on Micro Electro Mechanical Systems* (IEEE, 2005), pp. 666–669.
11. D. Braun and A. Libchaber, "Trapping of DNA by thermophoretic depletion and convection," Phys. Rev. Lett. **89**(18), 188103-1-188103-4 (2002).
12. S. Duhr and D. Braun, "Optothermal Molecule Trapping by Opposing Fluid Flow with Thermophoretic Drift," Phys. Rev. Lett. **97,** 038103-1-038103-4 (2006).
13. C. Farcau, H. Moreira, B. Viallet, J. Grisolia, and L. Ressier, "Tunable conductive nanoparticle wire arrays fabricated by convective self-assembly on nonpatterned substrates," ACS Nano **4**(12), 7275–7282 (2010).

14. C. V. Sternling and L. E. Scriven, “Interfacial turbulence: Hydrodynamic instability and the marangoni effect,” AIChE Journal **5**(4), 514–523 (1959).
15. Y. Zheng, H. Liu, Y. Wang, C. Zhu, S. Wang, J. Cao, and S. Zhu, “Accumulating microparticles and direct-writing micropatterns using a continuous-wave laser-induced vapor bubble,” Lab Chip **11**(22), 3816–3820 (2011).
16. A. S. Basu, and Y. B. Gianchandani, “Trapping and manipulation of particles and droplets using micro-toroidal convection currents,” in *Proceedings of IEEE Conference on Solid-State Sensors, Actuators and Microsystems* (IEEE, 2005), pp. 85–88.
17. A. Alexeev, T. Gambaryan-Roisman, and P. Stephan, “Marangoni convection and heat transfer in thin liquid films on heated walls with topography: Experiments and numerical study,” Phys. Fluids **17**(6), 062106 (2005).
18. E. Bodenschatz, W. Pesch, and G. Ahlers, "Recent development in Rayleigh-Bénard convection" Annu. Rev. Fluid Mech. **32**, 709–778 (2000).
19. V. Garcés-Chávez, R. Quidant, P.J. Reece, G. Badenes, L. Torner, and K. Dholakia, "Extended organization of colloidal microparticles by surface plasmon polariton excitation", Phys. Rev. B 73, 085417-1-085417-5 (2006).
20. G. M. Hale and M. R. Querry, “Optical constants of water in the 200-nm to 200-mm wavelength region,” Appl. Opt. **12**, 555-563 (1973).
21. S. Moon, “A novel double laser crystallization technique for producing location-controlled ultra-large polysilicon grain growth,” JKPS **47** (1), 133-141 (2005).
22. COMSOL documentation
23. R. Swanepoel, “Determination of the thickness and optical constants of amorphous silicon,” J. Phys E:Sci. Instrum. **16**, 1214-1222 (1983).
24. N. A. Bakr, A. M. Funde, V. S. Waman, M. M. Kamble, R. R. Hawaldar, D. P. Amalnerkar, S. W. Gosavi and S. R. Jadkar, “Determination of the optical parameters of a-Si:H thin films deposited by hot wire-chemical vapour deposition technique using transmission spectrum only,” J. of phys. **76**(3), 519-531 (2011)
25. A. M. Bakry, “Influence of Film Thickness on Optical Properties of Hydrogenated Amorphous silicon Thin Films,” Egypt. J. Solids, **31**(1), 11566 (2008).
26. A. V. Getling, *Rayleigh-Bénard Convection: Structures and Dynamics*, (World Scientific Publising, 1998).
27. D. R. Lide *CRC Handbook of chemistry and Physics* (CRC Press; 90th edition, 2009), chap 6
28. V. Arrizón, U. Ruiz, D. Sánchez-de-la-Llave, G. Mellado-Villaseñor, and Andrey S. Ostrovsky, “Optimum generation of annular vortices using phase diffractive optical elements,” Opt. Lett. **40**(7), 1173–1176 (2015).
29. R. Piazza and A. Parola, "Thermophoresis in colloidal suspensions," J. Phys.: Condens. Matter 20, 153102-1-153102-18 (2008)

1. Introduction

The manipulation of single cells and large biomolecules is a requirement of several medical and biological techniques from in vitro fertilization to genetic engineering. Nowadays, several techniques and devices for micromanipulation have been implemented to supplement the traditional approaches using micropipettes: optical tweezers [1] offer single particle manipulation but limited capacity to simultaneously trap large number of particles due to the strong focusing requirement; on the other hand dielectrophoresis [2] allows massive manipulation but lacks spatial resolution to manipulate individual particles. Several approaches have been proposed that combine both high-spatial selectivity and high throughput at the same time including optodielectrophoresis [3], spatial patterning of plasmonic [4], optofluidic [5], structured light landscapes [6, 7] among others. Recent works have shown that individual and collective trapping of large particles (hundreds of μm's in diameter) can be achieved by laser-induced convective flow using an absorbing thin film [8], resistive heating devices [9] or more complicated devices such as cantilevers [10]. These approaches are quite attractive because particles are captured over long ranges by the convection currents allowing, for example, concentration of DNA [11, 12] and direct assemble of nanoparticles [13]. In addition, free surfaces in liquid subject to thermal gradients may drive fluid motion due to the temperature-dependent surface tension. This effect is known as thermocapillary force or the thermal Marangoni effect [14]. Marangoni convection can be used to drive the motion of gas bubbles in liquids [15], liquid droplets in air [16] or thin films of fluids [17]. The other mechanism of convection is the Rayleigh-Bénard convection (RBC) which is the buoyancy-driven flow of a fluid heated from the lower substrate and cooled from the above one. Such flows result from the development of the convective instability if the static vertical

temperature gradient (the gradient that would be present in a motionless fluid under the same conditions) is large enough [18].
In this work, we exploit laser-induced convection currents to trap and manipulate silica microparticles, using power laser of up to 20 mW in order to avoid the formation of vapor bubbles as in previous reports [15]. In addition, interplay between convection currents and photophoresis lead to the formation of ring trapping zone around the beam. Finally, beam shaping by means of a Spatial Light Modulator (SLM) is used to convert a Gaussian beam into dynamic light rings that can efficiently employed to trap and manipulate in real time a large number of microparticles. Numerical simulations support qualitatively well our experimental findings. The interplay of convection currents and photophoresis has been studied before produced by surface plasmon polariton excitation for large-scale ordering and trapping of colloidal aggregations [19] and by absorption of light in liquids for DNA concentration [11,12]. Although similar results were obtained, important differences are highlighted here that allow real-time manipulation of a large number of microparticles with relatively low power. We achieve this through beam shaping the light used and demonstrate that the pattern of the force can be controlled by changing the light pattern, a result which is not immediately obvious due to the convection currents created and one which has not been reported before.

2. Laser-Induced Convection Current

The device employed consists of a colloidal suspension sandwiched between two glass plates (separated by ~100 μm). On one of the glass plates a thin film of amorphous silicon (a-Si:H) is deposited acting as the heating substrate. The absorption coefficient of the a-Si:H is very high (α_{aSi}~$2.77\text{x}10^4$ cm^{-1} at λ=532 nm) and therefore it is expected that a temperature gradient is created on the film and on the adjacent liquid. This temperature gradient drives convective flows, dragging the dissolved particles in water, and thus long-range capture of microparticles around the beam spot may be possible. In order to probe this assertion, numerical simulations were performed using finite element method (COMSOL) to solve the heat transfer and Navier-Stokes equations using the configuration shown in Fig 1a. Numerical results shows that temperature can reach up 100°C, so many parameters become temperature-dependent as shown in Table 1. Initial conditions assume a room temperature of 293.15 K, atmospheric pressure ($1\text{x}10^5$ Pa) and an initial motionless fluid.

Table 1. Material properties of water and amorphous silicon [20-22]

Material	k	ρ	c_p	α (λ=532nm)
	W/mK	kg/m^3	J/kgK	1/m
Water	$-0.87+9\text{x}10^{-3}T-1.6\text{x}10^{-5}T^2+8\text{x}10^{-9}T^3$	$838.47+1.4T-3\text{x}10^{-3}T^2+3.7\text{x}10^{-7}T^3$	$1.2\text{x}10^4-80.41T+0.31T^2-5.3\text{x}10^{-4}T^3+3.6\text{x}10^{-7}T^4$	$3.5413\text{x}10^{-2}$
a-Si:H	1.5	2330	992	$2.77\text{x}10^6$

Light absorption by the amorphous silicon produces a temperature gradient ∇T and then dissipative heating from a-Si: H, heats the water up according to the heat transfer equation;

$$\rho c_p u \cdot \nabla T = \nabla \cdot (k \nabla T) + Q \,. \tag{1}$$

In this equation steady-state condition is assumed, in addition, viscous heating and pressure work are ignored. Here ρ is the water density, c_p is its heat capacity, u is the fluid's field velocity, k is the thermal conductivity and $Q=\alpha I$ is the heat source (α is the absorption

coefficient and I is the optical intensity. The water's absorption coefficient is quite small compared to the a-Si:H one, so amorphous silicon acts as the only heat source.

The intensity distribution of the Gaussian beam inside the a-Si:H is given by

$$I_{aSi}(r,z) = T_{net}\frac{2P}{\pi w^2(z+z_0)}\exp\left(\alpha_{aSi}\left(z+l_{water}\right)\right)\exp\left(-\frac{2r^2}{w^2}\right) \qquad (2)$$

$$T_{net} = T_{air\text{-}glass}T_{glass\text{-}water}T_{water\text{-}aSi} \approx 0.63$$

where T_{net} is the net transmission which takes into account all Fresnel losses at the air-glass, ($T_{air\text{-}glass}$), glass-water ($T_{glass\text{-}water}$) and water-a-Si:H ($T_{water\text{-}aSi}$) interfaces, respectively. By taking a refractive index of n=3 for the a-Si:H at λ=532 nm [23-25], a total transmission of ~63% is found. l_{water} is the thickness of the water film, P is the beam power, and $w(z)$ is the beam radius defined as $w^2(z) = w_0^2\left[1+\left(\lambda\left(z+z_0\right)\right)^2/\left(\pi w_0^2\right)^2\right]$, where w_0 =5 μm is the beam waist at the distance z_0 = -95 μm i.e close to the a:Si-H film in accordance with the experiment. Figure 1b shows a typical temperature profile obtained by solving Eq.(1) with a heat source produced by a Gaussian beam, Eq-(2), using P=11 mW. At this power value, the water temperature around the focal point reaches the boiling point (~100°C) and so the formation of vapor bubbles is possible, as reported below. Note that the temperature inside the semiconducting film is higher (~120°C) than the boiling temperature. Note that due to heat diffusion, the region above the ambient temperature is larger than the beam spot. According to Eq.(1), the gradient temperature sets in motion the fluid at a velocity u, and since the water properties are temperature dependent, the appearance of buoyancy force and the creation of convection flows is expected. The Navier-Stokes equations describe how the velocity, pressure, temperature, and density of a moving fluid are coupled.

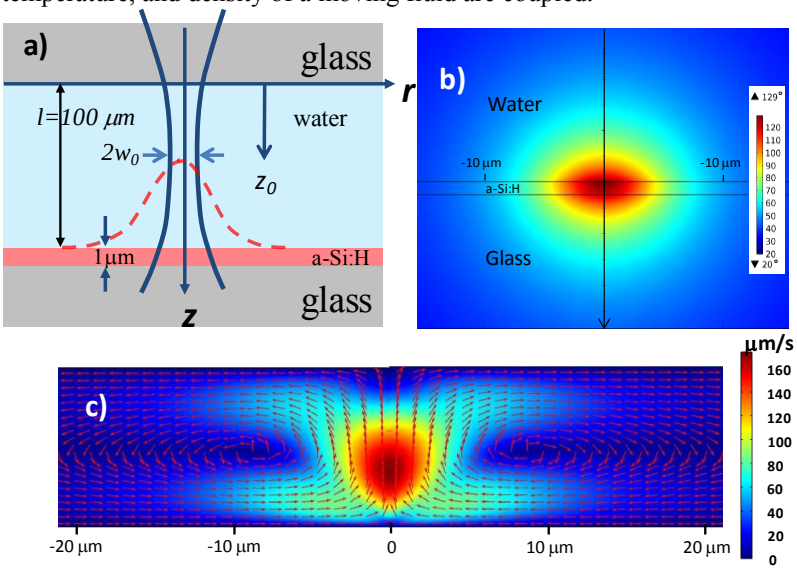

Fig. 1. a) Schematic of the model. The z=0 plane is placed at the glass-water interface and the beam waist is placed at a distance z_0 = -95 μm. The dashed line represents the thermal gradient produced by heating of the amorphous silicon film. b) Temperature obtained from Eq.(1) when a laser beam is focused on a thin absorbing film. See text for details; c) Typical velocity profile of the flow inside the water cell for the first 40 μm. The total length cell is 200 μm. The laser is focused at the center of the lower interface. The liquid moves upwards and then moves along the upper surface and the moves downwards at the edges and back towards the centre along the lower surface. Around ±10 μm a loop is created as indicated by the arrows.

The Navier-Stokes equations for an incompressible flow are

$$\rho(u\cdot\nabla)u = \nabla\cdot\left[-pI + \mu\left(\nabla u + (\nabla u)^T\right)\right] + F\,, \tag{3a}$$

$$\rho\nabla\cdot u = 0\,, \tag{3b}$$

where p is the pressure and F is a volumetric force. As volumetric force we used the buoyancy force $F = -g(\rho - \rho_0)$ responsible for the convection currents, with ρ_0= 998.3 kg/m^3 the water density at room temperature and ρ is the water density at the temperature T. Figure 1c shows the field velocity vector inside the liquid cell. Here only the first 40 μm around the focal point are shown although the total length of the cell is 200 μm. The calculated temperature inside the water scales linearly with laser power, as expected, according to the expression *T(P)=20°C + (7.11°C/mW)P* where *P* is the laser power in mW. Upper limit temperature is the water's boiling temperature (100°C) where the formation of bubbles is observed. This agrees with well with experiment. Depending on the applications, the peak temperature can be conveniently chosen to manipulate biological samples (<40°C to avoid damage) or inorganic particles where the upper limit is boiling of water. Note that the convective currents are directed upwards just above the hottest spot and then reaches the upper surface. The flow moves parallel to the upper substrate away from the center and directs towards the vertical walls (not shown) while at the lower substrate it moves parallel to the substrate towards the hot spot. According to Fig.1c, velocities of up to 160 μm/s are obtained near the beam spot, which agree quite well with experimental measurements. Around ±10 μm, a circulating zone is created more or less at middle of the cell. According to our numerical results, particles suspended in water will be dragged from regions far away from the laser beam and collected around it. In order to verify our results, a set of experiments were carried out and described below. The convective flow is neither Marangoni nor Rayleigh since no free surface is presented or the upper or lower substrate are cooled or heated uniformly. In addition, Rayleigh convection arises from an instability in a channel with a uniformly heated bottom surface when the Rayleigh number, Ra= $g\Theta\Delta T d^3/(\nu\kappa)$ exceeds a critical value of 1700 [26]. Here g is the gravity constant, d (beam diameter ~10 μm) is the characteristic length of the system, Θ (2.1×10^{-4} /°C [26]) is the thermal expansion coefficient, ν is the kinematic viscosity (0.001 cm^2/s and κ is the thermal diffusivity (1×10^{-3} /°C [27]). Such a system is quiescent until ∇T across the entire fluid cell is large enough to cause the instability. Assuming the extreme condition of ∇T =100°C then Ra<<1, i.e in principle, the buoyancy is much smaller than viscosity and heat diffusion dissipation.

2. Trapping and Manipulation Experiments

In order to perform the experiments we prepare a cell containing a colloidal solution of 2.5 μm diameter microparticles immersed in water and sandwiched between two glass coverslips separated by 100 μm thick plastic spacers. In one of the coverslips, 1 μm thick a-Si:H film was deposited. In order to create convection currents, a CW frequency doubled (Klastech, λ=532 nm, 1W) Nd:YAG laser was used to illuminate the film. The laser's power is controlled with a variable attenuator consisting of a λ/2 waveplate and a polarized cube beamsplitter. The laser beam is spatially filtered, collimated and directed towards a phase-only SLM (Holoeye PLUTO-VIS). The incidence angle between the SLM and the beam is Θ < 10° respect to the normal to ensure optimum phase modulation. A lens of focal length *f*=75 cm placed in front of the SLM is employed to Fourier transform the beam at its back focal plane, then the resulting beam is focused and imaged on the microparticles sample by a 60X microscope objective, as shown in Figure 2a. We consider two cases, *i)* the SLM is off, so that a Gaussian beam of approximately 10 μm in diameter was obtained on the sample; and *ii)* a synthetic phase hologram (SPH) is displayed on the SLM to shape the Gaussian beam.

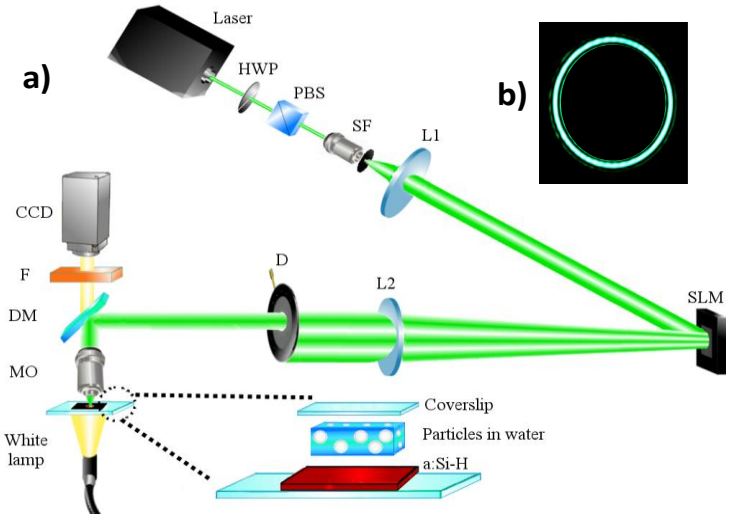

Fig. 2. a) Optical set up. A 1W, 532 nm laser is focused onto a 1μm a-Si:H film. The laser beam power is controlled with a half-wave plate (HWP) and a polarizing beam splitter (PBS), then the beam is spatial filtered (SP) and collimated with lens L1. After reflection on the SLM, the hologram is recovered by Fourier transform by lens L2. DM is a dichroic mirror, MO is 60x microscope objective. A white light source is used to illuminate the sample. The same objective is used to image the microparticles on the CCD camera. F is a filter that blocks the reflected green light to avoid CCD saturation, b) experimental image of the ring projected on the sample

The SPH is the binary phase modulation of the zero-order Bessel beam, $h=sign[J_0(2\pi\rho_0 r)]$, where the *sign* function takes the phase values π or $-\pi$, ρ_0 is the spatial frequency, and r is the radial coordinate. The transmittance of this SPH in the Fourier plane, which is realized by the lens L2, reshapes the Gaussian beam into a ring of radius $r_0=\lambda f\rho_0$ [28]. In Figure 2b, we show an experimental image of the reconstructed ring. A white light source is used to illuminate the sample and the trapped particles are imaged into a CCD camera with the same microscope objective. Finally, an optical filter was placed in front of the CCD camera to block the reflected green light to avoid camera saturation.

4. Results

4.1 Trapping by convection

Figure 3 shows snap shots of multiple particle trapping with a power of 0.8 mW. The broken line circle indicates the position of the laser beam. Note that particles are dragged from positions well beyond the field of view (~25x35) confirming the existence of convection currents. Optical trapping or electric field gradients due to space-charge redistribution, which is a possibility in amorphous semiconductors, are ruled out since they act nearby the laser beam. Since convection currents are symmetrically generated around the focal point, particles are collected around it. The average velocity of the particles is quite small ~ 2 μm/s, as a result, collecting a large number of particles takes more than 1 min. Note that at all times, the particle remains in focus at the substrate, indicating that the drag currents are weak and unable to overcome the gravity around the beam as the simulation indicates. Particles will continue to accumulate as long as the laser is on. In this way self-assembly of micro and nanoparticles is possible as shown in Ref 19.

One obvious disadvantage of this approach is the inability to trap particles in real time. Simulations indicates that the fluid velocity (and therefore particle velocity) increases linearly with power P as $v\cong 1.7(\mu m/mWsec)P$, where P is measured in mW. Experimentally, this is true below 3 mW obtaining a velocity of 4.7 μm/s at a power of 2.7 mW. However, for P>3 mW,

the particles are repelled from the beam's center creating a ring-trapping zone as shown in Figure 4.

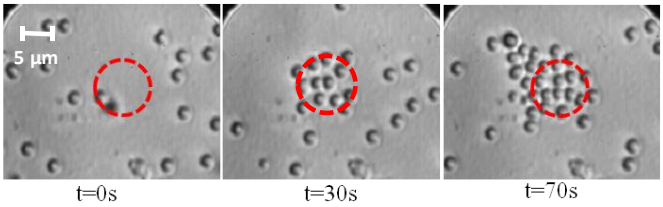

Fig. 3. Multiple trapping. Power of 0.8 mW, particles accumulated around the laser beam spot.

Also, note that particles in the ring move very fast in closed trajectories, as the particles are in and out of focus periodically (see Media 1). The diameter of ring-trapping zone is weakly dependent on power. Particles in the ring can be trapped and manipulated in two dimensions in real time. Similar results were reported in [15] but only on the presence of a vapor bubbles. This trapping and manipulation mechanism involving just convective drag forces and photophoresis and not relying on bubble formation is presented here for the first time to our best knowledge.

4.2 Trapping with vapor bubble

Further increase of the power above 11 mW, leads to the formation of vapor bubbles similar to those reported in [15]. Due to the high absorption of the film, low power laser (11 mW) can easily heat the water up to its boiling point and form vapor bubbles (Fig. 5). The trapping mechanism was attributed to the complex interplay of the temperature dependent superficial tension and convection currents. We notice that the temperature dependent surface tension remains as long as the vapor bubble subsists, as we continue observing trapping long before the laser beam has been turned off.

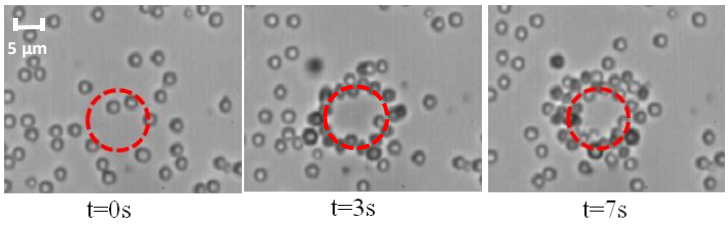

Fig. 4. Multiple trapping for power of 6 mW, the particles are trapped around of the area of the spot (Media 1).

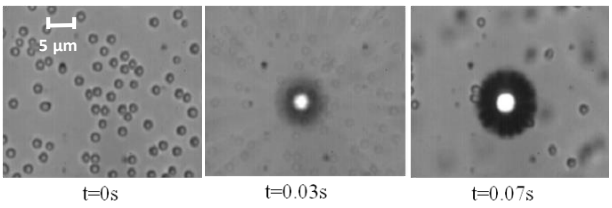

Fig. 5. Trapping by means of a vapor bubble. The particles are trapped to high velocity using 12 mW of laser power (Media 2).

5. Discussions

Our simulations describe qualitatively well the trapping (collection) of particles due to laser induced convection current showing that particles can be collected over the whole cell providing a mechanism for self-assembly of microparticles. Particles are dragged towards the

beam focus along the lower interface (a-Si:H) as they remain in focus at all times (depth of focus of 60x microscope objective ~1 μm). This is true even in the proximity of the beam where the velocity is the highest and directed upwards (see Fig.1). One possible reason is that gravity and radiation pressure prevent the particles from moving out of focus. Once the power is increased (between 3-11 mW), the particles are expelled from the beam center forming a re-circulation zone around the beam spot. It is worth to mention that in non absorbing substrates, like glass, this recirculating zone does not appears even at much higher powers. In addition, in glass substrates the particles are trapped by the transversal gradient force within the beam. Light absorption at a:Si-H heats up the water molecules increasing its kinetic energy while outside the beam its energy is smaller, i.e a gradient of temperature (see Fig. 1b) is produced. This means that particles within the temperature profile will be subject to non uniform forces i.e. thermo-photophoretic forces. So, particles in the beam will be expelled from hotter regions towards the coolest ones, at the same time convection currents drags particles towards the center of the beam forming a ring at the re-circulating zone. Although this recirculation zone in light-induced convection currents (see Fig 1c) is predicted by theory, it occurs in the middle of the cell. Besides it extend over 50 μm, which is well beyond depth of focus of our optics, while in the experiment the particles move no more than ~ 10 μm. Similar results were demonstrate in Refs. 11 and 12 where convection and photophoresis were produced by water absorption. The ring-trapping zone is achieved by modest increase on the water temperature (~2°C). It was shown that DNA concentration can by increased by several orders of magnitude in a ring centered on the laser beam where a gentle balance of convection and photophoresis is achieved. In our case, we produce much larger temperature gradients due the high absorption coefficient of a-Si:H. This is turns means that stronger convection and photophoretic forces allow the trapping and manipulation of micron sized particles as shown here and even hundred micron sized particles trapping [8] using modest power lasers. Garcés-Chávez et al showed that surface plasmon excitations activate convective forces that can be used to produce large-scale organization. Furthermore, they reduced vertical temperature gradients (and therefore convective forces) using a very thin cell (10 μm). By doing this, also large scale organization is produced by plasmonic forces. If the laser power is increased up to ~1 W, a ring trapping zone is produced as in our case by balance of plasmonic and photophoretic forces. We believe that this ring could have being observed in thick cell if they had increased the beam power. In our experiments a few mW of light is enough to provide real time manipulation using a much simpler and lower cost setup.

Modeling of thermophoretic forces is not an easy task, particularly in dense media since its amplitude is not only determined by the particle general bulk or surface physical properties (size, material density, thermal conductivity, or total surface charge) but rather it seems to be subtly related to the detailed microscopic nature of the particle/solvent interface [29]. Analytical solutions for the thermophoretic force in air exist (COMSOL include it in its library) but provide unrealistic (mm/sec) velocity in numerical simulations. Further modeling is outside of the scope of this paper since we are only interested on discussing the new manipulation mechanism.

So far we have shown that photophoresis expels the microparticles from the hotter towards the coolest regions. However, if the Gaussian beam is reshaped to produce complex beam profiles such as rings, Bessel or any other optical landscapes, different trapping configurations may be possible. Using this concept, a ring of light is produced as a result of a SPH of a Bessel beam as described in the experimental section. In this case, particles will be repelled symmetrically towards the ring's center. Outside the ring, the interplay of photophoresis and convective flow is still present as before. Approximately, 85 silica 2.5 μm particles in diameter are trapped simultaneously for a power of 18 mW (see Fig. 6). Note that although the power is larger than in the case of Gaussian illumination no vapor bubbles are produced because the local intensity is smaller than need it to reach vaporization. If power is increased beyond 20 mW, bubble formation and even thermocavitation can be observed.

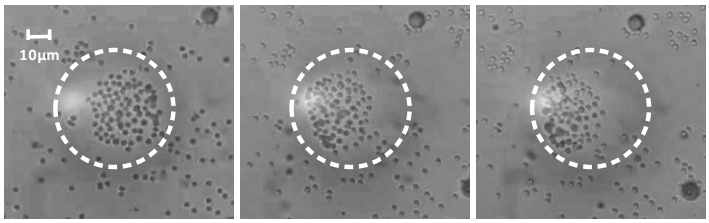

Fig. 6. Trapping with a ring-shapped light source generated with SPH. Particles are repelled by photophoresis towards the ring´s center. (Media 3).

Furthermore, since trapping is fast, dynamic light patterns can be implemented without the need of patterning heaters on the substrate [10]. The use of thermophoretic force to trap DNA by means of light ring was demonstrated by Duhr and Braun [12]. We went further by showing that massive simultaneous trapping and manipulation of microparticles is possible. In Figure 7, two examples of dynamic trapping with rings of light with different radius can be implemented to perform optical clearing (Fig 7a), or to collection of particles (Fig.7b). Note that in both cases when the ring is comparable to the heat diffusion length, microparticles near the ring center defocuses because vertical convective currents appear due to heat diffusion. This simple examples show that more complex configurations can be implemented in real time where operations like trapping, transport, and even sorting may be possible with SPH.

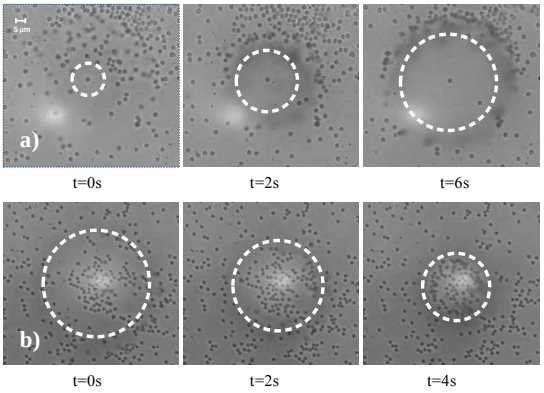

Fig. 7. Trapping with a dynamic ring-shaped light source generated with SPH: a) Optical clearing (Media 4) and b) Collecting and trapping particles (Media 5)

6. Conclusions

We have shown two dimensional trapping and manipulation can be achieved by convection currents using a low power lasers. For low power (0.8 mW) particles are trapped at the center of the beam but at higher powers (~3 mW) particles form a ring around the beam due to two competing forces: Stokes and thermo-photophoretic forces. Numerical simulations confirm that thermal gradients are responsible for the trapping mechanism. This technique offers a rich variety of trapping configurations. For example, illuminating the substrate with structured beams (rings, parallel lines, etc) could lead to the devices capable of performing an almost endless set of reconfigurable microparticle manipulations which combined the ability to move single cells or large biomolecules will produce a versatile and elegant life science tool.